Article:
Shahbazi, M, Rajabzadeh, G, Ettelaie, R et al. (1 more author) (2016) Kinetic study of k-carrageenan degradation and its impact on mechanical and structural properties of chitosan/ k-carrageenan film. Carbohydrate Polymers, 142. pp. 167-176. ISSN 0144-8617

https://doi.org/10.1016/j.carbpol.2016.01.037

Kinetic study of κ-carrageenan degradation and its impact on mechanical and structural properties of chitosan/κ-carrageenan film

Mahdiyar Shahbazi[a], Ghadir Rajabzadeh[b*], Rammile Ettelaie[c]

[a]Department of Food Chemistry, Research Institute of Food Science and Technology (RIFST), Mashhad, Iran.

[b]Department of Food Nanotechnology, Research Institute of Food Science and Technology (RIFST), Mashhad, Iran.

[c]Procter Department of Food Science, University of Leeds, Leeds LS29JT, United Kingdom.

ABSTRACT

The purpose of the current research was to study κ-carrageenan degradation behavior through thermal treatment, and its influence on chitosan/κ-carrageenan film properties. A pseudo first-order reaction equation was applied by using reciprocal plots of κ-carrageenan molecular mass versus heating time, which showed strongly heating time dependence. Incorporation of thermally treated κ-carrageenan to the chitosan had a deterioration effect on water resistance and water vapor permeability of the blend, in contrast to those for intact. A dramatic decrease of equilibrium moisture content and tensile strength were noticed, in which a longer time was found to be more effective. Furthermore, the contact angle of the films was found to be a function of the heating time. SEM revealed apparent agglomeration of κ-carrageenan through the thermal process. AFM demonstrated that the intact blend had the most flat surface, whilst the blend containing treated κ-carrageenan became rugged and uneven with high roughness.

*Corresponding author E-mail address: gh.rajabzaheh@rifst.ac.ir. Tel: +98(51)35425337. Fax: +98 (51) 35003150.

Keywords: Thermal depolymerisation, pseudo first-order reaction, Blend film, Equilibrium moisture content, Tensile strength, Surface roughness.

1. Introduction

The application of petroleum based packaging materials has a serious environmental pollution due to the fact that they are non-degradable (Hoagland & Parris, 1996). As an alternative, biodegradable materials from the natural sources like carbohydrates can be employed (Sanchez-Garcia, Hilliou, & Lagaron, 2010). However, a packaging based on carbohydrates suffers from poor physico-mechanical and weak barrier properties(Parris, Coffin, Joubran, & Pessen, 1995).

One way to resolve these problems is to blend the biopolymers to improve the film properties. These improvements could be ascribed to the strengthening of the mechanical parameters (Zhu, Sheng, & Tong, 2014; Zivanovic, Li, Davidson, & Kit, 2007), increasing the surface hydrophobicity (Zhu, Sheng, & Tong, 2014), decreasing the water vapour permeability (Zhu, Sheng, & Tong, 2014; Zivanovic, Li, Davidson, & Kit, 2007) and relative water resistance (Xiao, Gao, Wang, & Zhang, 2000).

Chitosan is distinguished as a natural polymer with wide applications in the food and pharmaceutical industries. Chitosan is one of the most abundant carbohydrates in the nature. It is obtained through the process of alkaline N-deacetylation of chitin, which is mainly extracted from the shellfish (Hoagland & Parris, 1996).This biopolymer has a semi crystalline structure and high hydrophilic characteristics, which can form hydrogen bonds with water molecules. A special feature of chitosan is the formation of uniform films with the potential applications in food industry (Xu, Kim, Hanna, & Nag, 2005). Chitosan becomes soluble and cationic when it is

dissolved in acidified solutions through organic acid, whereas most other hydrocolloids display anionic property in the solvents. So these soluble hydrocolloids become anionic in water, chitosan cation show well affinity for other hydrocolloids (Park, Lee, Jung, & Park, 2001).

Carrageenan is the sulfated form of D-galactan obtained from the red algae (Lobban, 1994). Carrageenan consists of repeating galactose units and 3, 6-anhydrogalactose joined by alternating α-(1, 3) and β-(1, 4) glycosidic links. All three kinds of carrageenan (iota, kappa and lambda) produce high viscosity when incorporated in the aqueous systems (Imeson, Phillips, & Williams, 2000). The kappa carrageenan (KC) is widely used for the synthesis of the blend films, where the physical and mechanical properties of the films are amended in the presence of KC.

Park, Lee, Jung, & Park (2001) prepared the blend film based on chitosan and KC in presence of several organic acids and found that the physical and mechanical properties of the blend film demonstrated strong dependency on the organic acid solvent. They results showed that the tensile strength and water barrier property of a blend of chitosan and KC involved acetic acid and ascorbic acid was significantly improved than other organic acid solutions.

There are several methods for preparing the biodegradable films based on the thermal processes, including thermo-compression, blow molding and solvent casting method (Fakhouri et al., 2013; Teixeira et al., 2012). The solvent casting, in particular, is widely used for the synthesis of the biodegradable films (Fakhouri et al., 2013). The temperature history of the biofilm has a great effect on the features of the film; however this effect has almost been completely ignored. More specifically, the depolymerisation kinetic by the thermal degradation during the preparation of the biodegradable films has rarely been evaluated.

In the aforementioned methods, whenever high temperatures were employed, the hydrolysis reaction occurred. Under these circumstances, degradation and scission of the chain caused a decrease in the molecular weight of polysaccharide chain (Bradley & Mitchell, 1988). In addition, the heat treatment highly affected the other dispersion parameters. It was proven that the degradation rates of the polysaccharides were related to their molecular conformation, in which the concentrated regions, in comparison with dilute regions, had a higher resistance to heat, and generally were more capable of hindering the chain degradation (Hjerde, Smidsrød, & Christensen, 1996).

As regards the systematic studies on the variables effect of the polysaccharide heat degradation and its influence on the film, these are scanty. The alteration of molecular mass and the mechanism of degradation via thermal casting method need to be explored in more details to fully understand their effects on the film properties.

Accordingly, the aim of this study is to investigate the changes in the molecular size of KC (using intrinsic viscosity as an indicator) occurring during being heated in aqueous media, and the incorporation of this biopolymer into the chitosan solution to evaluate the final resulting blend properties. For degradation rate of KC, our initial hypothesis is based on the fact that the chain scission of sulfate esters on the KC follows a pseudo first-order kinetics.

2. Materials and methods

2.1. Materials

The commercial potassium KC salt and chitosan were provided from Sigma-Aldrich chemical co. (St. Louis, MO, USA).

2.2. KC thermal treatment

Thermal treatment of biopolymers at 80°C is commonly used in the laboratory and industry for the preparation of their films. To investigate the degradation kinetic in this condition, KC (0.275 g, in accordance with critical overlap concentration) was completely dissolved in deionized water (0.275 g/dL) and heated at 80°C in a thermostatically controlled chamber under continuous stirring. This was followed by the thermal treatment at 60, 120, 180, and 240 min.

2.3. Rheological study of KC

After heat treatment, an Ostwald viscometer (Ubbelohde-type, Germany) equipped with a temperature control system was used to determine the coil overlap concentration (c*) of the KC chains and their intrinsic viscosity (40±0.1℃). The intrinsic viscosity ([η]) of KC was determined under the coil overlap concentration (in the dilute region). The sample viscosity (η) was converted to relative viscosity (η_{rel}), reduced viscosity (η_{red}) and inherent viscosity (η_{inh}) defined by Eqs. (1), (2) and (3), respectively:

$$\eta_{rel} = \frac{\eta}{\eta_0} = \frac{t}{t_0}.\frac{\rho}{\rho_0} \quad (1)$$

$$\eta_{red} = \frac{(\eta_{rel}-1)}{C} \quad (2)$$

$$\eta_{inh} = \frac{\ln(\eta_{rel})}{C} \quad (3)$$

where, t and t_0 are the efflux times of the solution and the solvent, ρ/ρ_0 is the ratio of the density of the solution to the used solvent, η_{rel}-1 is specific viscosity (η_{sp}), and C is the concentration of KC.

The $[\eta]$ is usually obtained from the mean intercept of $\frac{\ln(\eta_{rel})}{C}$ and $\frac{\eta_{sp}}{C}$ to the infinite dilution limit according to the Huggins (Eq. 4) and Kraemer (Eq. 5) empirical expressions:

$$\frac{\eta_{sp}}{C} = [\eta] + K_1[\eta]^2 C \quad (4)$$

$$\frac{\ln\eta_{rel}}{C} = [\eta] + K_2[\eta]^2 C \quad (5)$$

where, k_1 is the Huggins constant, which is 0.35 for KC (Harding, Day, Dhami, & Lowe, 1997; Huggins, 1942). K_2 is the Kraemer constant (Kraemer, 1938). Theoretically $k_1 + k_2 = 0.5$, so the Kraemer constant is 0.15 for KC (Morris & Ross-Murphy, 1981). All the tests were carried out in triplicate.

2.4. Theoretical Basis: Degradation Rate

Masson (1955) and Bradley & Mitchell (1988) illustrated that the chain scission of the glycosidic linkage of KC, for short-term heat treatment, is a first-order reaction. Based on this concept, the rate constant (r) of scission of KC can be determined upon heating process.

The degradation rate can be ascertained by using plots of reciprocal molecular mass against heating time. The rate constant of the degradation reaction can be determined by Eq. 6 (Masson & Caines, 1954; Bradley & Mitchell, 1988):

$$\left(\frac{1}{M_t}\right) - \left(\frac{1}{M_0}\right) = \left(\frac{r}{m}\right) t \quad (6)$$

where, M_t and M_0 (kDa) are the molecular weights at times t and t_0; r (min^{-1}) is the pseudo first-order rate constant; t is the heating time (min); and m (kDa) is the average molecular weight of monosaccharide units. On the hypothesis of Hjerde, Smidsrød, & Christensen (1996) and

Tanford (1961), α (1 → 3) and β (1 → 4) glycoside bonds on KC have a similar susceptibility to scission.

It is known that the intrinsic viscosity is correlated to molecular weight according to Marck-Houwink equation (Rao, 1999):

$$[\eta] = KM_w^{\alpha} \quad (7)$$

Combining Eqs. 6 and 7 provides a relationship between the time and intrinsic viscosity:

$$\left(1/[\eta]_t^{\frac{1}{\alpha}}\right) - \left(1/[\eta]_0^{\frac{1}{\alpha}}\right) = \left((r/m) \times K^{\frac{1}{\alpha}}\right) t \quad (8)$$

where, $[\eta]_t$ and $[\eta]_t$ are intrinsic viscosity at t and t_0; K and α are Marck-Houwink parameters, and $\left(r/m \times k^{\frac{1}{\alpha}}\right) t$ is the slope of the curve.

As mentioned above, the degradation is a pseudo first-order reaction at the short-term heat treatment. The relationship of the inverse [η] versus time is then expressed by Eq. 9:

$$\left(1/[\eta]_{n+1}^{\frac{1}{\alpha}}\right) - \left(1/[\eta]_n^{\frac{1}{\alpha}}\right) = \left((r_n/m) \times k^{\frac{1}{\alpha}}\right) t \quad (9)$$

Here, the subscripts n+1 and n are $(n+1)^{th}$ and $(n)^{th}$ data during prolonged time, respectively, and now (t) is the time duration between these two data steps.

The reported values for K and α in the literature were 2.09×10^{-4} and 0.78, respectively (Vreeman, Snoeren, & Payens, 1980). The molecular weight (m) for the KC monosaccharide was also considered to be 0.192 kDa. All the tests were carried out in triplicate.

2.5. Preparation of chitosan/KC film

The synthesis of the chitosan/KC film was based on a solution casting method and evaporation process. The neat chitosan film solution was made by dispersing 1 g chitosan in 2% v/v of the acetic/ascorbic acids aqueous solution to obtain a concentration of 2 g/dL. The solution was stirred at 60^{o}C for 20 min.

The base intact blend film was prepared by the addition of 0.275 g of KC in the 1 g/dL of the chitosan solution and vigorous stirring at 60^{o}C for 20 min.

The KC solutions were, subsequently, treated at the various thermal times as described in section 2.2, and were then mixed with chitosan solution to obtain treated blend film. The samples were coded as T_{60}, T_{120}, T_{180} and T_{240}, in which superscript implies the dissolution time of the KC at 60, 120, 180 and 240 min, respectively. The constant temperature of 80^{o}C was considered for all treatments.

Finally, 20 ml of the each solution was poured into the plates and placed in the oven for 18 h. The films were peeled off the glass plates and were conditioned for 36 h at ambient temperature and 45% RH for further experiments.

2.6. Physical properties

2.6.1. Equilibrium moisture content (EMC)

The films were stored at ambient temperature during three days in desiccators with saturated salt solutions (including LiCl, $KC_2H_3O_3$, $MgCl_2$, K_2CO_3, NaBr, NaCl, KCl and KNO_3) to generate relatively specified humidities (about 11- 94% RH). After conditioning, the dried films

were weighed at regular intervals before being transferred to a cup container and dried at 105°C for 24 h. The EMC was determined by measuring the weight loss percentage of films as specified by Eq. 10.

$$EMC = \frac{M_W - M_d}{M_d} \quad (10)$$

In the above equation, M_w and M_d are wet and dry base weight, respectively.

GAB (Guggenheim–Anderson–de Boer) model was applied to fit film sorption isotherm data, and monolayer values for moisture were calculated from the equations. GAB isotherm model can be expressed as follows:

$$m = \frac{m_0 C K a_w}{(1 - K a_w)(1 - K a_w + C K a_w)} \quad (11)$$

where, M is the equilibrium moisture content at a water activity aw, m_0 is the monolayer value, and C and k are the constants.

2.6.2. Water solubility (WS)

The total soluble matter was exhibited as the percentage of the dry matter of the film solubilized in distilled water after 24 h immersion. The films (5×5 cm) were dried at 105°C for 24 h. Then, they were transferred into a flask and shaken on a rotary shaker for 24 h. Following this, the specimens that remained insoluble were removed from the water and dried at 105°C for 24 h. WS values were determined according to Eq. 11:

$$WS = \frac{S - S_0}{S_0} \quad (12)$$

where, S_0 is the initial and S the insoluble dry matter weight. The results of all the experiments were analyzed in triplicate and the mean and standard deviation of the data were reported.

2.6.3. Water vapour permeability (WVP)

The barrier property of the films was determined by gravimetric method (ASTM, 1995b). Each specimen was attached to a cup (containing silica gel) in a chamber. The RH of the chamber was fixed at 76.1% with a saturated salt solution of NaCl at 40°C. The weight of each cup was regularly recorded for 18 h. The slop of the weight gain versus time represents water vapor transmission rate (WVTR). The WVP (g/m.s.P) was obtained according to Eq. 12:

$$WVP = \frac{WVTR \times L}{\Delta P} \quad (13)$$

where, L is film thickness (mm) and ΔP (Pa) water partial pressure difference between two sides of the film. All the tests were carried out in triplicate and the mean and standard deviation of the data were reported..

2.7. Mechanical Properties

The mechanical parameters of the film were obtained by using a texture analyzer (Texture Analyzer, TA-XT_2, UK) based on the ASTM standard method D882-88 (ASTM, 1989a). The distance grip separation was set at 60 cm and the grip speed was set at 10 cm/s. The films (8×1 cm) were preconditioned at 25°C and RH 50% for 24 h. The tensile strength (TS) was determined from the maximum force on a cross section of rectangular specimens. Elongation at break (EB) was obtained from the initial change in the length (6 cm). All the data were analyzed by Exponent Lite software (version 6.1.4). All the tests were performed in triplicate.

2.8. Morphological behavior analysis by SEM

The surface morphology of the film was evaluated by using Hitachi SEM (model S-2830N). The incorporation of KC to the neat chitosan film and the effect of thermal treatment on the morphological and integrity of the films were assessed from SEM micrographs. The specimens were coated with a thin layer of gold and a 20X magnification was used. The energy levels were applied in the range of 15-20 KV in order to avoid damaging to the samples.

2.9. Surface topography

The topography of the films was analyzed by a Digital Instrument atomic force microscope (DI Nanoscope TV, NY) equipped with an E-scanner. Tapping mode with nominal spring constant of 20–100 N $m^{-1}$and nominal resonance frequencies of 10–200 kHz were used. The device was operated in tapping mode with topography scan size in the range 1 µm×1 µm. The software NanoScope v 5.31r1 (Veeco Software) was used to calculate the roughness value of the films.

2.10. Surface hydrophobicity

The contact angle (CA) was measured with a contact anglemeter (OCA 20, Dataphysics). The film was transferred into the flat surface and 5 µm drops of deionized water with a Hamilton syringe (100 µm, Hamilton, Switzerland) placed on the film. The CA was recorded using natural light after 30 s. The images were analyzed by Dino Lite Pro software.

2.11. Statistical analysis

The completely randomized design (CRD) was used for all experiments. Each measurement was analyzed by ANOVA. The mean and standard deviation of the experimental results were calculated using SPSS software with $p<0.05$ (Version 19, SPSS Inc., Chicago, IL).

3. Results and discussion

3.1. Coil overlap point and intrinsic viscosity of KC

The c* of KC was determined by plotting specific viscosity [η_{sp}] versus concentration as shown in Fig. 1. A sharp slope change in the [η_{sp}] of KC at 0.275 g/dL, represents the coil overlap point. In a dilute region, the curve had an approximately linear trend, which could be described by the spatially separate individual coils of the biopolymer. As concentration of the biopolymer was increased, the [η_{sp}] value increased logarithmically, where the separate chains become entangled with each other. The macromolecule conformation upon coil overlapping was altered as the chains became increasingly entangled (Morris, 1992).

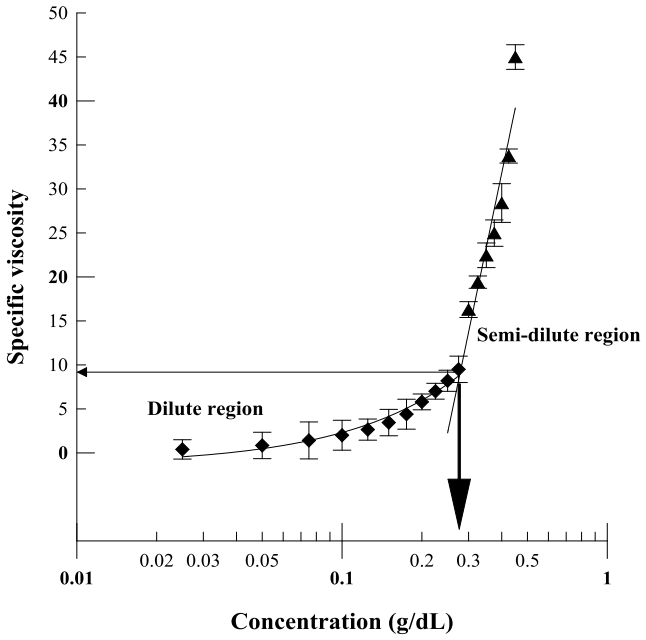

Fig. 1 . The change of specific viscosity of KC versus concentration at various heating times.

A convenient index of the hydrodynamic volume of the biopolymer coils is the limiting viscosity number or intrinsic viscosity (Morris, Cutler, Ross-Murphy, Rees, & Price, 1981). The intrinsic viscosity ([η]) is obtained in the dilute region below the c* of the biopolymer. The extent of [η] for KC was derived from the average intercepts for reducing viscosity and inherent viscosity (that are predicted by Eqs. 2, 3, 4), according to the method of Huggins and Kraemer, respectively. The extent of intrinsic viscosity for KC was calculated to be around 14.19 dL/g, which was much higher than values of 10.4 and 6.3 dL/g that previously reported by Vreeman, Snoeren, & Payens (1980) and Harding, Day, Dhami, & Lowe (1997), respectively.

3.2. KC coil overlap parameter

The occupancy degree of the hydrodynamic volume of all coils in the biopolymer solution can be characterized by the coil overlap parameter regardless of its type and molecular weight (Morris, Cutler, Ross-Murphy, Rees, & Price, 1981). The coil overlap parameter or c[η] basically

consists of the intrinsic viscosity and biopolymer concentration, which can be taken as a measure of the effective volume function of the polymer chains at specific concentration of C.

The typical double logarithmic plot of the $(\eta_{sp})_0$ against $c[\eta]$ is presented in the Fig. 2. The critical coil overlap parameter ($c^*[\eta]$) can be obtained from this plot, where onset of the chain entanglement is clearly observed. The extent of $c^*[\eta]$ was determined to be approximately 3.903, which shows $(\eta_{sp})_0$=9.5 at the intersection point. Morris, Cutler, Ross-Murphy, Rees, & Price (1981) showed a similar behavior for the several different random coil polysaccharides; also, they found out that more generally $c^*[\eta]\approx4$. The slope of zero-shear specific viscosity plotted against $c[\eta]$ at the dilute region i.e. $c[\eta]<c^*[\eta]$, is around 2.58, while it is 8.53 in the semi-dilute, $c[\eta]>c^*[\eta]$, regime.

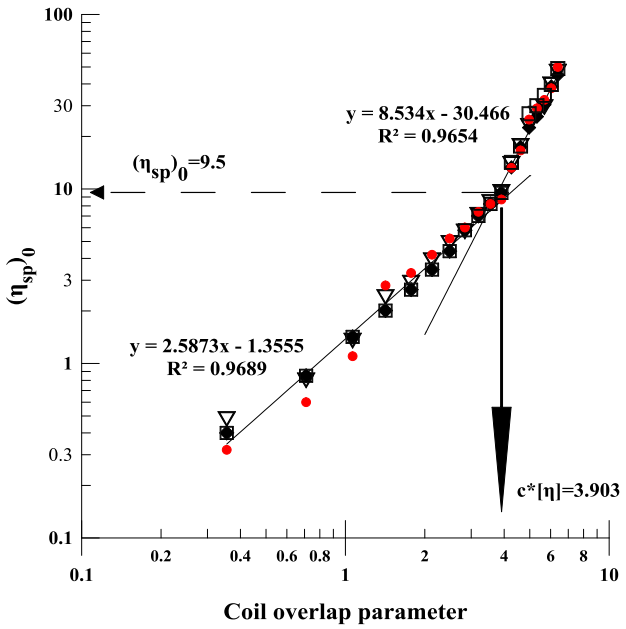

Fig. 2. Variation in the 'zero shear' viscosity of KC with the degree of occupancy of space by the chain coils. The results are shown for KC treated at: intact (●), 60 min (△), 120 min (▽) 180 min (□), and 240 min (♦).

Another factor that is important for the later experiments is the susceptibility of the c*[η] with regard to the thermal treatments. Fig. 2 also shows that the c[η] is essentially independent of the heating time. The lack of changes in c*[η] upon heating time reflects the independence of the coil overlap parameter to the time of thermal treatment. Bradley & Mitchell (1988) found out that sodium alginate at 25^{o}C and 102^{o}C had approximately the same intrinsic viscosity and explained that the point of the coil overlap was independent of the temperature. De Vasconcelos, De Azevedo, Pereira, & Fonseca (2000) were also revealed that the coil overlap of potato starch appeared in c≈1.5 dL/g in the temperature range of 0-45^{o}C.

3.3. Degradation rate of KC

The extent of KC degradation was conducted by measuring the changes of intrinsic viscosity (as an indicator of the molecular mass degradation) versus heating time. Fig. 3 displays exponential decrease of the [η] by extending the heating time. As can be seen, the [η] values for 0, 60 and 120 min were 14.19, 12.80 and 11.90 dL/g, respectively. Further heating time from 180 to 240 min was associated with the decreasing of intrinsic viscosity from 9.2 to 6.6 dL/g. This phenomenon could be attributed to the decrease in the average molecular weight, which increases the molecule's compactness and radius of gyration.

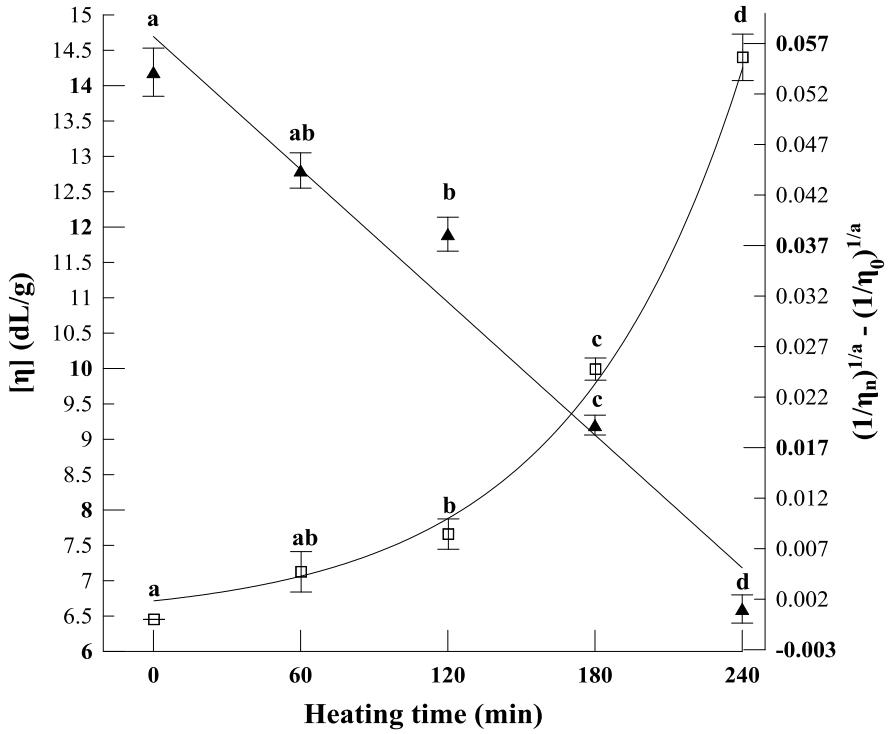

Fig. 3. Changes in intrinsic viscosity and $\left(1/[\eta]_t^{\frac{1}{\alpha}}\right) - \left(1/[\eta]_0^{\frac{1}{\alpha}}\right)$ of KC upon various heating times.

Fig. 3 is also plotted based on the conception that the degradation rate of KC is the pseudo first-order kinetics. The degradation rate obtained by plotting $\left(1/[\eta]_t^{\frac{1}{\alpha}}\right) - \left(1/[\eta]_0^{\frac{1}{\alpha}}\right)$ versus heating time, which its slope, $\left((r/m) \times [k]^{\frac{1}{\alpha}}\right)$, having a positive trend. The time dependency of the experiment can be expressed by the degradation rate upon heating time. The increase of the inverse intrinsic viscosity caused by increasing the heating time from 60 to 240 min was associated with increase of $\left(1/[\eta]_t^{\frac{1}{\alpha}}\right) - \left(1/[\eta]_0^{\frac{1}{\alpha}}\right)$ from 0.023 to 0.16 dL/g. This is fully in accord with the linearity of thermal degradation, implying the validity of the Eq. (8) for assessing the degradation rate upon the thermal treatment.

The increasing of the heating time is coincident with a faster reduction of the $\left((r/m) \times [\eta]_{MH}^{\frac{1}{\alpha}}\right)$, especially at longer times, where it causes a decrease in [η]. This is due to a scission of the chains at 3,6-anhydrogalactose linkage (Masson, 1955; Hjerde, Smidsrød, & Christensen, 1996), and if the long-period time is employed, degradation will occur at a broader level. Hydrolysis reaction (Bradley & Mitchell, 1988; Singh & Jacobsson 1994; Karlsson & Singh, 1999) and thermal degradation (Masson, 1955; Bradley & Mitchell, 1988) are two different hypotheses generally proposed to explain this phenomenon, as a result of the molecular chain degradation and reduction of MW.

The r_n was derived from the slope of $\left(1/[\eta]_{n+1}^{\frac{1}{\alpha}}\right) - \left(1/[\eta]_{n}^{\frac{1}{\alpha}}\right)$ versus the heating time. There is a linear relationship between r_n and $[\eta]_n$ for the short times during the thermal treatment (Fig. 4). This is determined by Eq. 8 and confirms that the degradation rate depends especially on the intrinsic viscosity. The thermal degradation rate was recognized to follow a pseudo first-order kinetic and mainly, depended on the molecular weight.

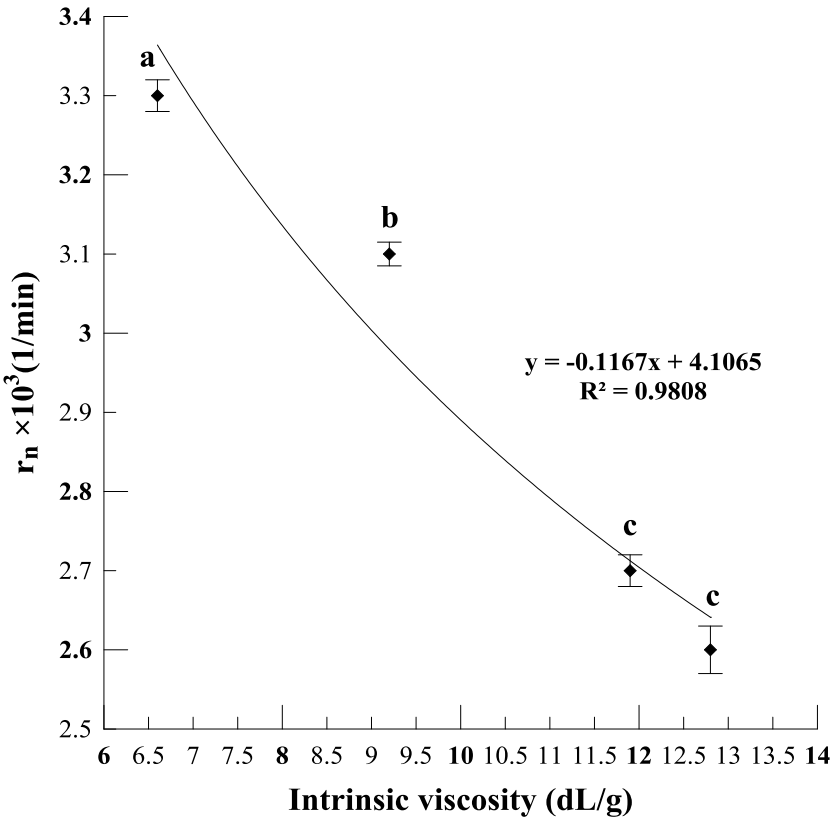

295

296

297 **Fig. 4 .**Changes of degradation rate constant (r_n) against $[\eta]_n$ at which r=0 ($[\eta]_{r=0}$)

298 3.4. Physical properties of the films

299 3.4.1. Characterization of the films

300 The appearance of the neat chitosan film (with no plasticizer) was opaque, non-flexible and
301 brittle. This phenomenon was proven by the lack of plasticizer, where it was capable of forming
302 a substantially more flexible and soft film. After blending chitosan with untreated KC, the film
303 was seen to be more flexible with a smooth and uniform surface.

304 According to thickness results, there was no important difference between thickness value of
305 the neat chitosan and T_{60}-T_{180} films, which all films have a value in range of 56.6-58.0 µm.

306 There is a notably difference in the thickness value of T_{240} film. In the recent case, the thickness
307 value was determined approximately 45.4 µm, which was considerably less than the neat
308 chitosan film.

309 3.4.2. Water solubility (WS)

310 The water solubility depends on the film constitution, molecule conformation, and thermal
311 condition (Gennadios, Ghorpade, Weller, & Hanna, 1996; Pérez-Gago, Nadaud, & Krochta,
312 1999). From the results of the ANOVA test, the WS of the blend film was significantly
313 influenced by the presence of KC (Table 1). The chitosan film has low water solubility, 27.3%,
314 due to its highly crystallized and rigid structure. The WS value of the chitosan film more
315 decreased to 23.3% after incorporating with intact KC. The linkage of the hydrophilic chains
316 between chitosan and KC led to a relatively stiffer structure, which decreased the accessibility of
317 the water to the hydrophilic groups. The increase of the water resistance results from KC
318 blending was reported in the several previous studies. Rhim (2012) was found that the WS of the
319 agar film was notably decreased through increasing the KC content.

320 The effect of heating time on the solubility of the films is also shown in Table 1. The WS of
321 blend films decreased as the period of the thermal treatment increased up to 120 min and, after
322 that, increased. The comparison of WS of the neat chitosan film and T_{120} exhibited a reduction
323 by more than 32.3%. About T_{180} and T_{240}, the solubility increased linearly to 23.6 and 26.7%,
324 respectively. It emanated from the partial degradation of KC, which resulted in decreasing in the
325 hydrophilic site of KC for interaction with chitosan.

326 **Table 1.** Summary of the physico- mechanical and structural properties of the films.

Film type	WS (%)	WVP (g/m.s.Pa)×10^{-10}	TS (MPa)	EB (%)	Contact angle (°)	Roughness parameters	
						R_q (nm)	R_a (nm)
Chitosan	27.3±0.6[a]	0.62±0.002[a]	8.1 ± 0.4[a]	24.41 ±0.1[a]	39.0±1.7[a]	19.11	10.83
Intact blend	23.3±1.1[b]	0.51±0.003[b]	13.2±0.7[b]	17.83± 0.2[b]	67.8±2.2[b]	8.24	6.15
T_{60}	22.8±1.0[b]	0.43±0.001[c]	16.8 ± 0.3[c]	14.48 ± 0.1[c]	68.2±1.4[b]	7.10	4.90
T_{120}	18.5±0.5[c]	042±0.002[c]	17.6 ± 0.3[c]	14.25± 0.2[c]	50.2±0.8[c]	8.94	6.40
T_{180}	23.6±0.9[b]	0.49±0.002[b]	17.1 ± 0.2[c]	14.2 ±0.2[c]	51.4±1.1[c]	16.57	11.89
T_{240}	26.7±0.7[a]	0.58±0.001[d]	13.6 ± 0.3[b]	17.1± 0.3[b]	41.5±1.6[b]	37.95	23.00

[a–d] Means (three replicates) within each column with different letters are significantly different (p<0.05), Duncan's test.

3.4.3. The equilibrium moisture content (EMC)

The films should be capable of withstanding the atmospheric humidity effect. Hence, the determination of EMC is essential in the packaging applications. The EMC data of the films were fitted to GAB models and isotherms are presented in Fig. 5. In general, the moisture sorption isotherms for the all films displayed a sigmoidal curvature and shown that the EMC increased gently with an increase in relative humidity up to 57.5%, afar which there is a sharp increase in the EMC in the film samples. The sigmoidal curvature trend of the EMC is well recognized in the literature for most food materials, including carbohydrates (Srinivasa, Ramesh, Kumar, and Tharanathan, 2003). At RH of 90%, the neat chitosan film had an initial EMC of about 40.5%, which rose up to 47.1%, when incorporated with intact KC. The KC had a high hydration capacity at the critical overlap point (0.275 g/dL). This led the intact blend to have an increased moisture affinity at a higher value of RH. The increase in the water uptake of the blend film by increasing the KC previously reported. In a study conducted through Rhim (2012) an increase in the moisture content of the agar film was observed after KC blending.

As shown in Fig. 5, the EMC kinetic curves of the T_{120} and T_{180} samples followed the same trend as untreated sample. The kinetic curves of T_{120} and T_{180} were slightly higher when compared with the untreated blend and T_{60} films. The EMC of the T_{240} was dramatically reduced down to 36.6% in RH of 90%. This indicates that at higher RH, the T_{240} sample had much lower tendency to water uptake, in comparison with the other films, as a result of KC chain degradation during 240 min thermal treatment.

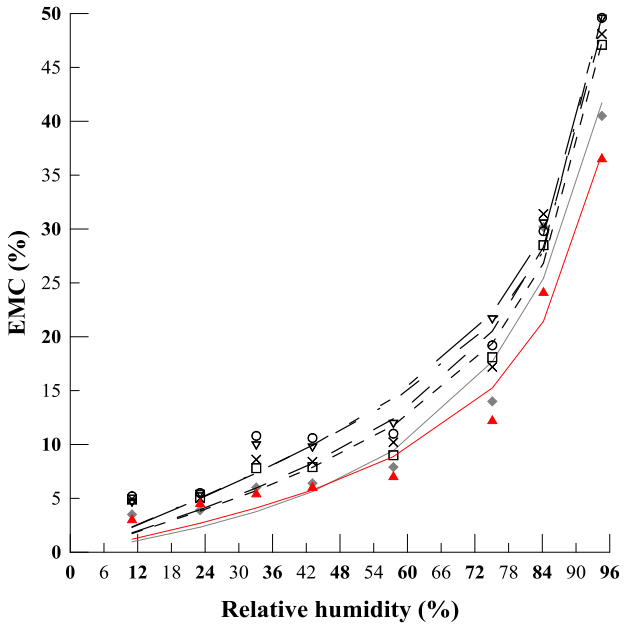

Fig. 5. The kinetic curves of EMC against RH% of the chitosan film during heat treatment: pure chitosan (♦), intact blend (□), T_{60} (×), T_{120} (∇), T_{180} (○), and T_{240} (▲).The lines were derived from the GAB equation

Calculated GAB model constants, coefficient of determination (r^2) and Fit standard error are summarized in Table 2. High r^2 and low standard error values endorsed that the GAB model was a suitable model for the experimental data. Mathematical fitting of EMC data to GAB model exhibited that the monolayer values (M_0) were influenced by both incorporation of KC and thermal treatments. The highest monolayer values were belonged to T_{120} and T_{180} samples about

1.22 and 1.73 gH_2O/g solids, respectively. The monolayer value shows the amount of water, adsorbing in a single layer to binding sites in the sample. The incorporation of KC makes more active sites, where water molecules could be adsorbed through exposing the hydrophilic groups to the film surface. The monolayer values decreased drastically as thermal time treatment increased, where the T_{240} sample showed the lowest monolayer value (0.27 g H_2O/g solids) among all treated films. The C parameter in the thermally treated film decreased with increased the thermal time, except T_{240} film.

Table 2. GAB model constants and coefficient of determination (r^2) and fit standard error for various films.

Film type	Thickness (µm)	M_0*	C**	K**	r^2	Fit standard error
Chitosan	57.6±0.7[a]	0.082	1.13	0.85	0.983	0.030
Intact blend	57.2±0.6[a]	0.56	0.29	0.94	0.993	0.022
T_{60}	58.0±0.7[a]	0.53	0.32	0.92	0.989	0.029
T_{120}	57.4±1.1[a]	1.22	0.18	0.95	0.995	0.018
T_{180}	56.6±0.4[a]	1.73	0.12	0.98	0.991	0.025
T_{240}	45.4±14[b]	0.27	0.43	0.91	0.988	0.022

*Monolayer moisture content in g H_2O/g solids.
**GAB constant.

3.4.4. Water vapour permeability (WVP)

The assessment of the possibility of water vapour penetration rate between the products in the packing and outer perimeter can be determined by WVP. In the case of food products, the evaluation of WVP is crucial (Robertson, 2012). The WVP values of the films are represented in Table 1. It is clearly obvious that the change of WVP does not follow a special trend. The WVP

372 of the intact blend, T_{60} and T_{120} declined, while WVP increased in the case of T_{180} and T_{240},
373 compared with the chitosan film.

374 The WVP of chitosan films decreased from 0.62 to 0.51 ($\times 10^{-10}$ g/m.s.Pa), after blending with
375 untreated KC. This improvement can be ascribed by the formation of hydrogen bond between
376 chitosan and KC, which results in the formation of a relatively tough structure. This occurrence
377 leads to a barrier against moisture movement (Xu, Kim, Hanna, & Nag, 2005). Park, Lee, Jung,
378 & Park (2001) were synthesized a blend film constituted by chitosan and KC and measured
379 WVP of this blend. Their works showed that the water barrier properties notable increased by
380 about 31%. In a favorable study, a linear relationship for WVP of the chitosan/starch film was
381 found, in which an increase of chitosan content led to a decrease in the WVP (Xu, Kim, Hanna,
382 & Nag, 2005).

383 The WVP for T_{60} and T_{120} was lower in comparison to both the chitosan and the intact blend
384 film. No significant difference was observed between the T_{60} and T_{120} samples ($p<0.05$). Table 1
385 shows that the WVP values of T_{180} and T_{240} films increased linearly with KC incorporation. The
386 highest WVP was found for the T_{240}, which represented a slight resistance to the vapour
387 transition through the film. The massive decomposition and degradation of KC chains during 240
388 min heat treatment could affect the hydrophilic sites, which weakened the interaction between
389 the chitosan and KC. So, the film formed no rigid structure to block the passage of moisture
390 transport.

391 3.5. Mechanical properties

392 Tensile strength (TS) is an important property and defines the resistance of the film to rupture
393 when material is submitted to the tensile force.

394 The TS and elongation at break (EB) were convenient parameters for the evaluation of the
395 mechanical behavior of the film. The changes of TS as a function of thermal treatment are shown
396 in Table 1. A remarkable increase in the TS was observed by the incorporation of intact KC into
397 the chitosan film. This increase is due to mainly the formation of hydrogen bonding in the intact
398 blend, which provided a firm structure in comparison to the neat chitosan film. Park, Lee, Jung,
399 & Park (2001) reported that TS of the chitosan film after introducing KC strongly increased from
400 initial value 3.8 to 25.5 MPa in the presence acid acetic and acid ascorbic 1%. In contrast, in the
401 other work performed by Rhim (2012), the addition of KC could not improve the TS of the agar
402 based film.

403 A notable increase in TS was also observed with samples of T_{60}-T_{180}. The statistical difference
404 in TS value between these films was not significant ($p<0.05$). Conversely, the thermal treatment
405 had an obvious effect on the TS in the case of T_{240} film. The extent of film TS after 240 min was
406 associated with a decrease to the 20.6 MPa. The reduction of TS can be attributed to the
407 diminishing of the reaction sites of KC for intramolecular interactions.

408 From the results of the mechanical test, the EB of the neat chitosan film considerably
409 decreased after introducing intact KC (Table 1). It was observed that the extent of EB of the
410 chitosan film dropped from 24.41% to 17.83% in regard to the untreated blend. According to the
411 inverse relation between TS and EB, it was evident that with the increase of the TS, as seen
412 above, the extent of EB would reduce. This finding was similar to Park, Lee, Jung, & Park
413 (2001) who reported a noteworthy reduction in the resilience of the chitosan film after
414 incorporating of KC. In the case of films that contained treated KC, the EB decreased with the
415 increasing of thermal treatment time up to a certain value, and then began to increase. For T_{60}-
416 T_{180} films, the EB decreased significantly compared to the chitosan and intact blend films

417 ($p<0.05$). In contrast, EB of the T_{240} sample reached 17.1% and, thus, was similar to that of the
418 intact blend.

419 3.6. Structural properties

420 3.6.1. Surface morphology

421 The SEM image of the films is shown in Fig. 6. As can be seen, the neat chitosan film
422 involved an irregular morphology with some cracks on the surface (Fig. 6 a). This might have
423 been due to the lack of the plasticizer in the preparation of the neat chitosan film. The plasticizers
424 are generally polyols that are incorporated into the biopolymer chains. They can rupture the
425 hydrophilic bonds, leading to the separation of the chains, which increase the flexibility and the
426 resilience of the film.

427 The most prominent effect of introducing KC into the chitosan film was the disappearance of
428 the cracks. The SEM micrographs revealed a smooth morphology without any fracture for the
429 intact chitosan/KC blend film (Fig. 6 b).

430 The heat treatment severely affected the integrity and morphological structure of the films,
431 except for T_{60} sample (Fig. 6 c). The flat morphology of the film was affected more and more by
432 increasing the heating time. The surface morphology of T_{120}, T_{180} and T_{240} films became rugged
433 and uneven with agglomerated pieces apparent in the SEM micrographs, among which, the T_{240}
434 surface seemed to be more affected by the thermal treatment (Fig. 6 d-f).

435
436
437
438
439
440

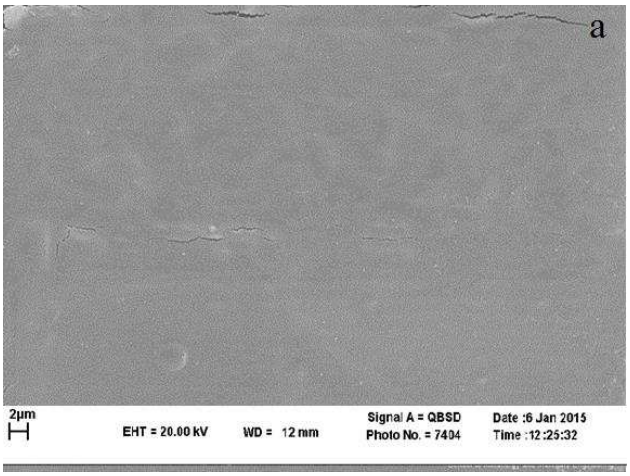

441
442
443

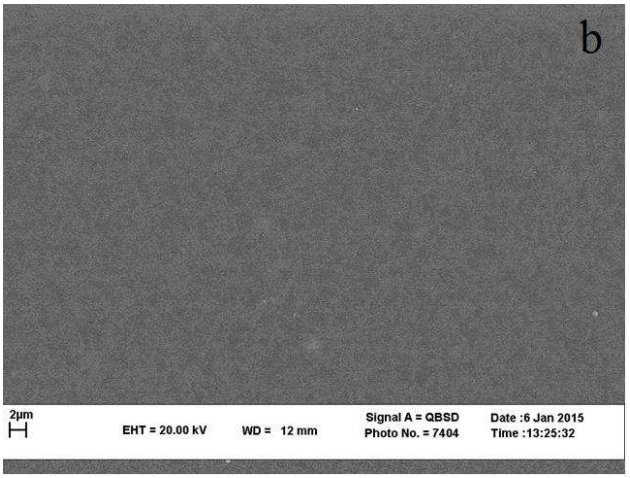

444

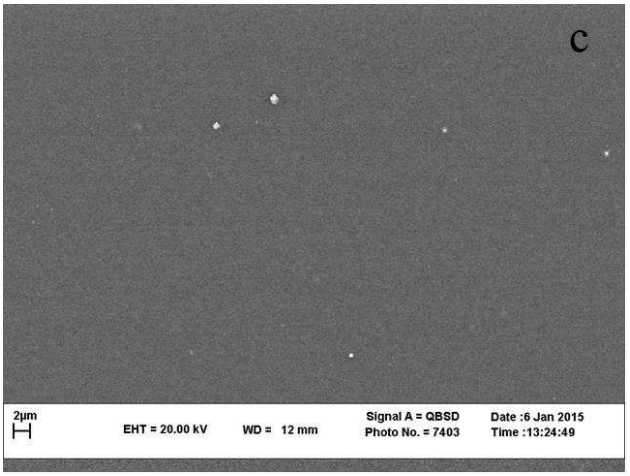

445
446

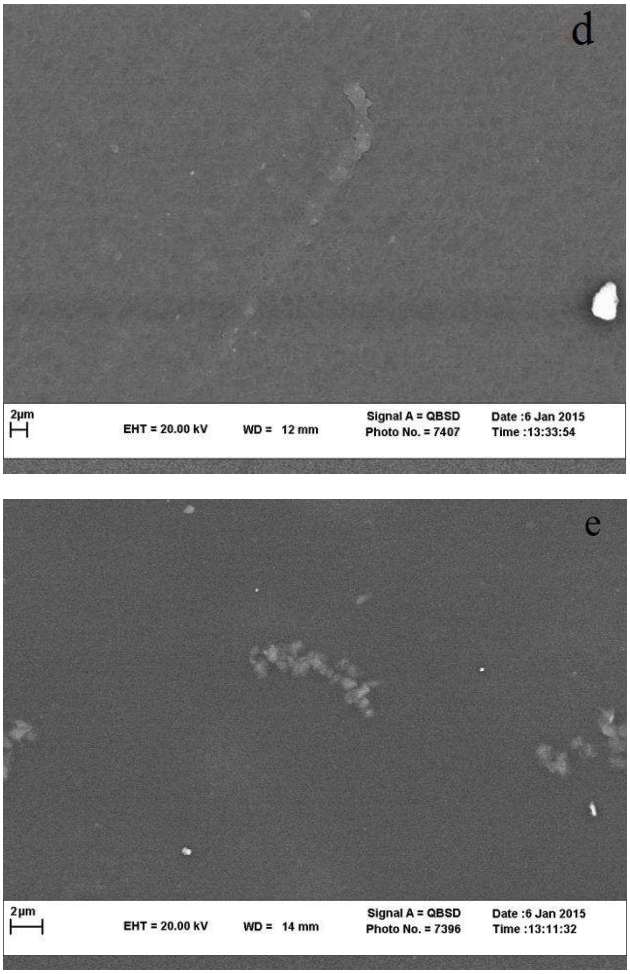

Fig. 6. SEM micrographs of the films: (a) pure chitosan; (b) intact blend; (c) T_{60}; (d) T_{120}; (e) T_{180} and (f) T_{240}, at magnification of ×10000.

3.6.2. Surface roughness

The AFM analysis was used to provide a better understanding of the surface topography of the films. AFM obtained reliable qualitative and quantitative information as three-dimensional topographical parameters in the nanometer scale.

Fig. 7 represents three-dimensional characteristics of various films and shows the remarkable differences between the film types. As expected, the surface topography of the neat chitosan

458 film, obtained from SEM images, was somewhat rough, heterogeneous and with surface
459 irregularities. The film surface became smooth as KC was incorporated. The topography of both
460 untreated blend and T_{60} films was uniform and homogenous.

461 The roughness parameters, such as average roughness (R_a) and root mean square roughness
462 (R_q), were obtained. The first of these quantities expressed that the average of absolute value of
463 height deviations from the mean surface, and the second was a measure of the root mean square
464 average of height deviations from the mean plane. As can be seen in Table 1, the intact blend and
465 T_{60} films showed low values of R_a and R_q, with no notable differences in AFM parameters. The
466 T_{120} film exhibited a fair degree of irregularity on the surface, which reflected the effect of the
467 thermal treatment on the film. The T_{120} film had high values of R_a (8.94 nm) and R_q (6.40 nm) in
468 comparison to the untreated blend and T_{60} films. As mentioned in section 3.3, thermal treatment
469 seemed to alter the KC matrix and caused a high extent of chain degradation. This, in turn,
470 brought about particle aggregation or flocculation.

471 The topography of the film surfaces was greatly accentuated, when the thermal time was
472 applied at higher levels. Further AFM imaging at T_{180} and T_{240} film clearly showed the presence
473 of grooves and cracks on the surface of the films. All the parameters showed a prominent
474 increase in the degree of roughness for the T_{180} and T_{240} samples. The roughness parameters of
475 T_{240} were even more than the neat chitosan film. The roughness observed on the surface of the
476 T_{240} film, was indicative of a degradation of the KC chains, in accordance with the earlier
477 hypothesis that implied chains hydrolysis at the higher temperatures.

478

479

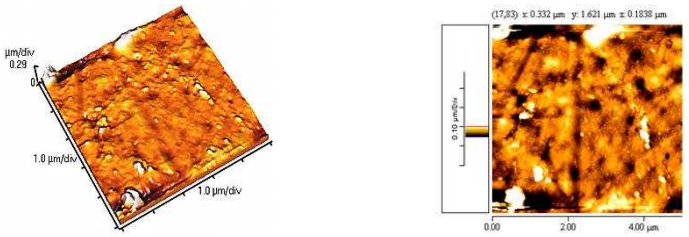

Neat chitosan film

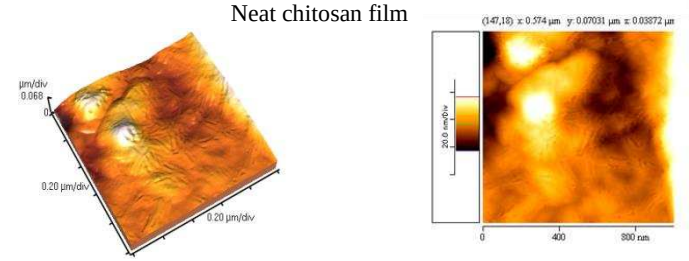

Intact blend film

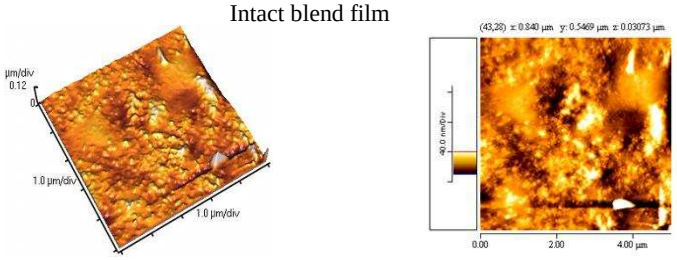

T_{60} sample

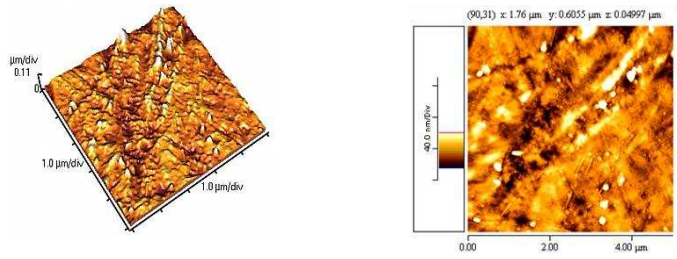

T_{120} sample

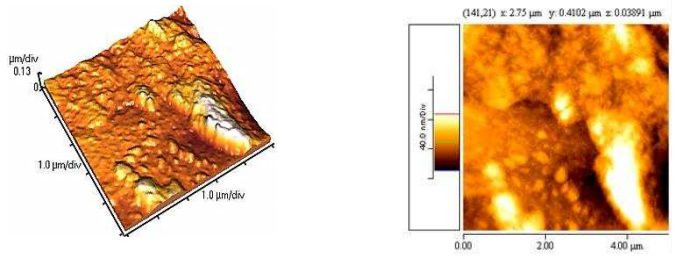

T_{180} sample

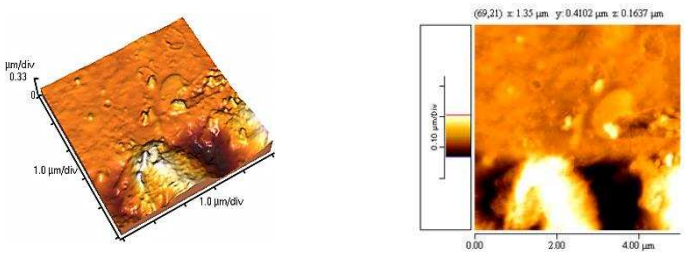

T_{240} film

Fig. 7. Typical AFM topography images of the films.

3.6.3. Contact angle (CA)

The changes in the surface hydrophobicity of the film were evaluated by the measurement of the water droplet contact angle and data are summarized in Table 1. The CA of the neat chitosan film exhibited a moderately low contact angle of θ=39°, which the droplet completely absorbed into the neat chitosan after 1 min. The rough surface and hydrophilic backbone of the chitosan chains caused its surface to be highly hydrophilic and wettable (Table 1). The CA data for the intact blend film revealed that KC improved the surface hydrophobicity of the pure chitosan film. A considerable increase by 29° was observed in the intact chitosan/KC film. This improvement essentially resulted from the disappearance of the surface cracks. On the other hand, the incorporation of surface hydroxyl groups by forming hydrogen bond in the untreated blend led to further rigidity of the film and lesser hydrophilic sites on the film surfaces. This was in agreement with the results obtained from both physical and mechanical properties, as was described in sections 3.4 and 3.5.

The influence of various heating times on the CA of the films can also be seen in Table 1. The surface hydrophobicity of the T_{60} film was similar to the intact blend film (θ=68.2°). It was observed that the magnitude of CA decreased gradually for T_{120}, T_{180} and T_{240} films. Among the films that have undergone thermal treatment, T_{240} was accompanied by the highest decrease in

520 the value of CA. From the topographic images, (Fig. 7), it was revealed that the surface of the
521 heat treated film was very uneven and the surface roughness is dominant factor that altered the
522 CA.

523 **4. Conclusion**

524 This study demonstrates that the film preparation using the thermal casting method enhances
525 the potential of the polysaccharide degradation, which impacts on the film properties. The
526 existence of a linear relationship between k_n and $[\eta]_n$ indicates that the thermal degradation of
527 KC follows a pseudo first-order kinetics, and it depends on its molecular weight. The order of
528 susceptibility to the thermal degradation by the various thermal time treatments resembles the
529 results on the other kind of hydrolysis reactions. It was found out that thermal treatment had
530 influenced the film characteristics, especially in its water solubility, mechanical and structural
531 properties. Incorporation of KC (at the level of coil overlap) to the chitosan solution also led to a
532 significant improvement in the physico-mechanical properties. More precaution should be taken
533 to limit the thermal degradation of polysaccharides during thermal casting method.

534 **References**

535 Bradley, T., & Mitchell, J. (1988). The determination of the kinetics of polysaccharide thermal
536 degradation using high temperature viscosity measurements. Carbohydrate Polymers, 9(4),
537 257-267.

538 De Vasconcelos, C., De Azevedo, F., Pereira, M., & Fonseca, J. (2000). Viscosity–temperature–
539 concentration relationship for starch–DMSO–water solutions. Carbohydrate Polymers, 41(2),
540 181-184.

541 Fakhouri, F. M., Costa, D., Yamashita, F., Martelli, S. M., Jesus, R. C., Alganer, K., Collares-
542 Queiroz, Innocentini-Mei, L. H. (2013). Comparative study of processing methods for
543 starch/gelatin films. Carbohydrate Polymers, 95(2), 681-689.

544 Gennadios, A., Ghorpade, V., Weller, C. L., & Hanna, M. (1996). Heat curing of soy protein
545 films. Biological Systems Engineering: Papers and Publications, 94.

546 Harding, S. E., Day, K., Dhami, R., & Lowe, P. M. (1997). Further observations on the size,
547 shape and hydration of kappa-carrageenan in dilute solution. Carbohydrate Polymers, 32(2),
548 81-87.

549 Hjerde, T., Smidsrød, O., & Christensen, B. E. (1996). The influence of the conformational state
550 of κ-and τ-carrageenan on the rate of acid hydrolysis. Carbohydrate Research, 288, 175-187.

551 Hoagland, P. D., & Parris, N. (1996). Chitosan/pectin laminated films. Journal of agricultural
552 and food chemistry, 44(7), 1915-1919.

553 Huggins, M. L. (1942). The viscosity of dilute solutions of long-chain molecules. IV.
554 Dependence on concentration. Journal of the American Chemical Society, 64(11), 2716-2718.

555 Imeson, A., Phillips, G., & Williams, P. (2000). Carrageenan. Handbook of hydrocolloids, 87-
556 102.

557 Karlsson, A., & Singh, S. K. (1999). Acid hydrolysis of sulphated polysaccharides. Desulphation
558 and the effect on molecular mass. Carbohydrate Polymers, 38(1), 7-15.

559 Kraemer, E. O. (1938). Molecular weights of celluloses and cellulose derivates. Industrial &
560 Engineering Chemistry, 30(10), 1200-1203.

561 Lobban, C. S. (1994). Seaweed ecology and physiology: Cambridge University Press.

562 Masson, C. (1955). The Degradation Of Carrageenin: I. Kinetics in aqueous solution at pH 7.
563 Canadian Journal of Chemistry, 33(4), 597-603.

564 Masson, C., & Caines, G. (1954). Viscosity and molecular weight of degraded carrageenin.
565 Canadian Journal of Chemistry, 32(2), 51-58.

566 Morris, E. (1992). Physico-chemical properties of food polysaccharides Dietary Fibre—A
567 Component of Food (pp. 41-56): Springer.

568 Morris, E. R., Cutler, A., Ross-Murphy, S., Rees, D., & Price, J. (1981). Concentration and shear
569 rate dependence of viscosity in random coil polysaccharide solutions. Carbohydrate Polymers,
570 1(1), 5-21.

571 Morris, E., & Ross-Murphy, S. (1981). Techniques in carbohydrate metabolism. B310, 1.

572 Park, S. Y., Lee, B. I., Jung, S. T., & Park, H. J. (2001). Biopolymer composite films based on κ-
573 carrageenan and chitosan. Materials Research Bulletin, 36(3), 511-519.

574 Parris, N., Coffin, D. R., Joubran, R. F., & Pessen, H. (1995). Composition factors affecting the
575 water vapor permeability and tensile properties of hydrophilic films. Journal of agricultural
576 and food chemistry, 43(6), 1432-1435.

577 Pérez-Gago, M., Nadaud, P., & Krochta, J. (1999). Water vapor permeability, solubility, and
578 tensile properties of heat-denatured versus native whey protein films. Journal of Food Science,
579 64(6), 1034-1037.

580 Rao, M. (1999). Introduction: intrinsic viscosity. Rheology of fluid and semisolid foods, 12-14.

581 Rhim, J. W. (2012). Physical-Mechanical Properties of Agar/κ-Carrageenan Blend Film and
582 Derived Clay Nanocomposite Film. Journal of Food Science, 77(12), N66-N73.

583 Robertson, G. L. (2012). Food packaging: principles and practice: CRC press.

584 Sanchez-Garcia, M. D., Hilliou, L., & Lagaron, J. M. (2010). Nanobiocomposites of
585 carrageenan, zein, and mica of interest in food packaging and coating applications. Journal of
586 agricultural and food chemistry, 58(11), 6884-6894.

587 Singh, S. K., & Jacobsson, S. P. (1994). Kinetics of acid hydrolysis of κ-carrageenan as
588 determined by molecular weight (SEC-MALLSRI), gel breaking strength, and viscosity
589 measurements. Carbohydrate Polymers, 23(2), 89-103.

590 Srinivasa, P., Ramesh, M., Kumar, K., & Tharanathan, R. (2003). Properties and sorption studies
591 of chitosan–polyvinyl alcohol blend films. Carbohydrate Polymers, 53(4), 431-438.

592 Tanford, C. (1961). Physical chemistry of macromolecules: Wiley.

593 Teixeira, E. d. M., Curvelo, A. A., Corrêa, A. C., Marconcini, J. M., Glenn, G. M., & Mattoso, L.
594 H. (2012). Properties of thermoplastic starch from cassava bagasse and cassava starch and their
595 blends with poly (lactic acid). Industrial crops and products, 37(1), 61-68.

596 Vreeman, H., Snoeren, T., & Payens, T. (1980). Physicochemical investigation of k-carrageenan
597 in the random state. Biopolymers, 19(7), 1357-1374.

598 Xiao, C., Gao, S., Wang, H., & Zhang, L. (2000). Blend films from chitosan and konjac
599 glucomannan solutions. Journal of Applied Polymer Science, 76(4), 509-515.

600 Xu, Y., Kim, K. M., Hanna, M. A., & Nag, D. (2005). Chitosan–starch composite film:
601 preparation and characterization. Industrial crops and products, 21(2), 185-192.

602 Zhu, G., Sheng, L., & Tong, Q. (2014). Preparation and characterization of carboxymethyl-
603 gellan and pullulan blend films. Food hydrocolloids, 35, 341-347.

Zivanovic, S., Li, J., Davidson, P. M., & Kit, K. (2007). Physical, mechanical, and antibacterial properties of chitosan/PEO blend films. Biomacromolecules, 8(5), 1505-1510.